

Multifunctional Antibacterial Nanonets Attenuate Inflammatory Responses through Selective Trapping of Endotoxins and Pro-Inflammatory Cytokines

Nhan Dai Thien Tram, Quy Thi Ngoc Tran, Jian Xu, Jeannie Ching Ting Su, Wupeng Liao, Wai Shiu Fred Wong, and Pui Lai Rachel Ee*

Extracellular lipopolysaccharide (LPS) released from bacteria cells can enter the bloodstream and cause septic complications with excessive host inflammatory responses. Target-specific strategies to inactivate inflammation mediators have largely failed to improve the prognosis of septic patients in clinical trials. By utilizing their high density of positive charges, *de novo* designed peptide nanonets are shown to selectively entrap the negatively charged LPS and pro-inflammatory cytokines tumor necrosis factor- α (TNF- α) and interleukin-6 (IL-6). This in turn enables the nanonets to suppress LPS-induced cytokine production by murine macrophage cell line and rescue the antimicrobial activity of the last-resort antibiotic, colistin, from LPS binding. Using an acute lung injury model in mice, it is demonstrated that intratracheal administration of the fibrillating peptides is effective at lowering local release of TNF- α and IL-6. Together with previously shown ability to simultaneously trap and kill pathogenic bacteria, the peptide nanonets display remarkable potential as a holistic, multifunctional anti-infective, and anti-septic biomaterial.

1. Introduction

Following antibiotic-induced lysis and cell death, Gram-negative bacteria release membrane-bound lipopolysaccharides (LPS) into the bloodstream.^[1] Unchecked systemic inflammatory responses to endotoxemia can result in collateral damage to host tissues and disruptions to physiological processes, potentially leading to septic shock with a high mortality rate.^[2] Thus far, efforts to develop target-specific therapies against sepsis has been thwarted by the dynamic interplay among structurally diverse pro-inflammatory and anti-inflammatory agents of both host and microbial origins.^[3] In general, antibodies targeting individual cytokines have not yielded promising outcomes in treating septic patients in clinical trials.^[4] More recent works have explored the feasibility of simultaneously capturing multiple key inflammatory mediators

by exploiting the common abundance of negative charges on LPS and human pro-inflammatory cytokines,^[5–7] with synthetic cationic nanoconstructs of diverse materials and morphologies reported.^[5,8]

Inspired by the trap-and-kill immune defense strategy ubiquitous in nature, our group recently designed synthetic β -hairpin antimicrobial peptides (AMPs) with the ability to self-assemble into amyloid-like nanonets specifically in response to bacterial endotoxins.^[9] These peptide nanonets, which comprise extensively cross-linked nanofibrils, displayed unique trap-and-kill dual-functionalities, which present a direct upgrade from the trap-only nanonets in nature which are reliant on other host immune components for antimicrobial activity.^[10] Upon coming into contact with LPS, the peptide can either: (1) undergo fibrillation to form cross-linked nanonets for physical trapping of nearby bacteria cells,^[9] or (2) fold into hairpin conformations for membranolytic antimicrobial activity.^[11] The side strands of our peptides carry three Leu–Lys repeat units, and the resulting polycationicity proved integral to facilitating interactions between the peptides and endotoxins. As such, we hypothesized that our fibrillating peptides could display anti-inflammatory functionality by capturing free endotoxins and pro-inflammatory cytokines in solution via electrostatic attractions. Selective trapping of pro-inflammatory cytokines is highly coveted for

N. D. T. Tram, J. Xu, J. C. T. Su, P. L. R. Ee
National University of Singapore
Department of Pharmacy
18 Science Drive 4, Singapore 117543, Singapore
E-mail: phaepir@nus.edu.sg

Q. T. N. Tran, W. Liao, W. S. F. Wong
National University Health System
Department of Pharmacology
Yong Loo Lin School of Medicine
16 Medical Drive MD3, Singapore 117600, Singapore

Q. T. N. Tran, W. S. F. Wong
Drug Discovery and Optimization Platform (DDOP)
Yong Loo Lin School of Medicine
National University Health System
Singapore 117600, Singapore

Q. T. N. Tran, W. Liao, W. S. F. Wong
Singapore-HUJ Alliance for Research and Enterprise (SHARE)
1 CREATE Way, Singapore 138602, Singapore

 The ORCID identification number(s) for the author(s) of this article can be found under <https://doi.org/10.1002/adhm.202203232>

© 2023 The Authors. Advanced Healthcare Materials published by Wiley-VCH GmbH. This is an open access article under the terms of the Creative Commons Attribution-NonCommercial License, which permits use, distribution and reproduction in any medium, provided the original work is properly cited and is not used for commercial purposes.

DOI: 10.1002/adhm.202203232

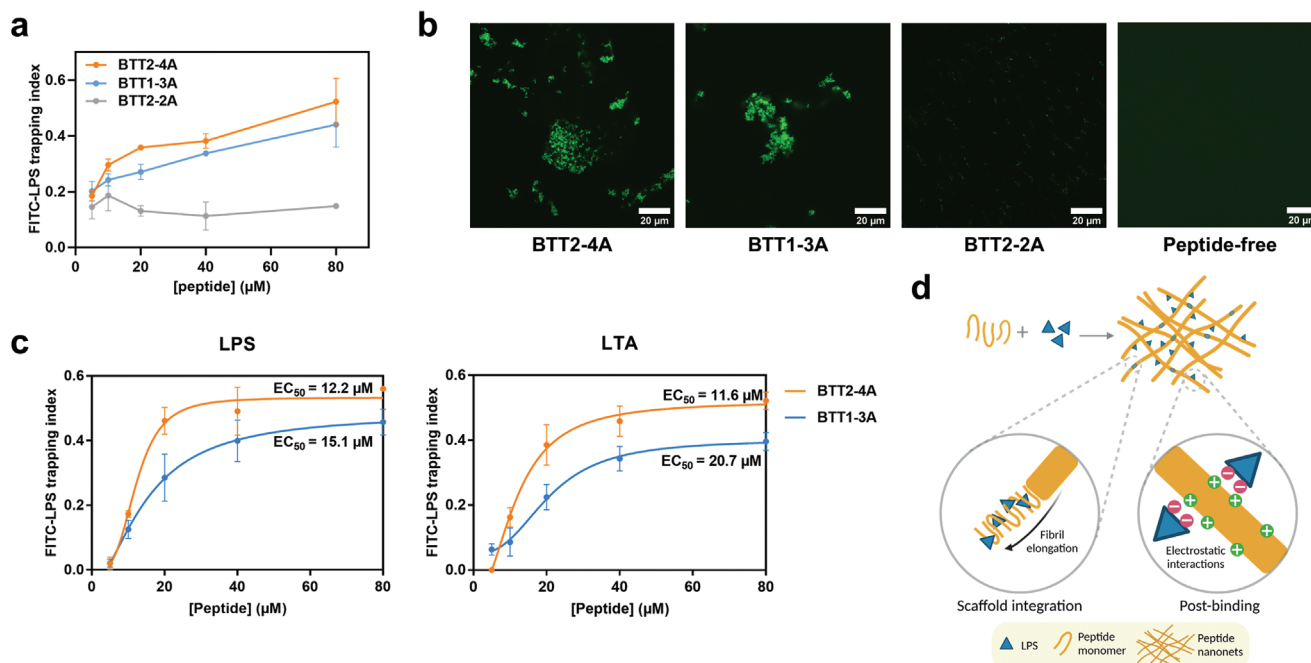


Figure 1. Peptide nanonets entrap LPS via two different mechanisms. a) FITC-LPS trapping index of peptide was computed by measuring fluorescence emission of FITC-LPS in the supernatant ($\lambda_{\text{EX}} = 488 \text{ nm}$ and $\lambda_{\text{EM}} = 520 \text{ nm}$) after 1 h of incubating LPS ($2 \mu\text{g mL}^{-1}$) with peptide at different concentrations. b) Confocal microscopy images of $64 \mu\text{m}$ peptide incubated with $32 \mu\text{g mL}^{-1}$ FITC-LPS for 1 h. Magnification = 200x. Scale bar = $20 \mu\text{m}$. c) FITC-LPS trapping index of pre-formed nanonets was determined after 1 h pre-incubation with LPS or LTA ($2 \mu\text{g mL}^{-1}$) followed by 1 h incubation with FITC-LPS ($2 \mu\text{g mL}^{-1}$). For (a) and (c), three repeats were conducted in duplicates and data were expressed as mean \pm SE, and data points were fitted to a non-linear regression inhibitor concentration versus response model for computation of EC_{50} values. d) Proposed dual mechanism of LPS trapping by the peptide nanonets via scaffold integration and post-binding.

sepsis management, given the complex concoction of pro- and anti-inflammatory cytokines typically faced in a cytokine storm. Endotoxin trapping can impede its engagement with host immune and endothelial cells, including activation of toll-like receptor 4 (TLR4) and induction of nitric oxide production.^[12,13] By alleviating the damage of endotoxemia, our multifunctional nanonets potentially offer a holistic anti-infective therapy that mitigates both upstream and downstream ramifications of infectious pathogenesis. As the first report of multifunctional peptide nanonets, we believe this work will help accentuate the clinical potential of this class of biomaterials. In comparison to recently explored anti-septic strategies for capturing endotoxins and cytokines (e.g., bioengineered extracellular vesicles,^[7] and telodendrimer nanotrap),^[5] the synthesis of our short linear peptides is far more streamlined with well-established solid-phase peptide synthesis approach. In addition, our system offers superior flexibility as specific functionalities of the nanonets can be readily fine-tuned through simple manipulation of the peptide sequence, as illustrated in both this manuscript and prior works from our group.^[9,11]

2. Results and Discussion

2.1. Peptide Nanonets Bind and Entrap Bacterial Endotoxins

From our in-house library of β -hairpin AMPs,^[9,11] we selected two representative fibrillating peptides previously demonstrated to display potent trap-and-kill activity against pathogenic bacteria,

BTT1-3A and BTT2-4A, for investigating their anti-inflammatory activity, as compared to the non-fibrillating peptide BTT2-2A. Their sequence and properties are listed in Table S1, Supporting Information. As shown in transmission electron microscopy images (Figure S1, Supporting Information), BTT2-4A formed expansive nanonets selectively in the presence of bacterial LPS, but not buffer alone. To study the in vitro LPS-trapping ability of the nanonets, we employed a fluorescence assay using fluorescein isothiocyanate (FITC)-labeled LPS.^[6] After incubating the peptides with FITC-LPS for 1 h, nanonets self-assembled through stacking of the peptide monomers with LPS molecules acting as amyloid-nucleating sites, thus capturing the LPS in solution. The sample was then centrifuged to pellet the nanonet-bound LPS, and the amount of free LPS in the supernatant was measured via FITC fluorescence for calculating the FITC-LPS trapping index. A higher index reflects greater LPS-trapping efficacy. As expected, the fibrillating BTT2-4A and BTT1-3A displayed higher FITC-LPS trapping indices than the non-fibrillating BTT2-2A, in a concentration-dependent manner (Figure 1a). LPS-trapping efficacy of BTT2-4A (0.52 at $80 \mu\text{M}$) was moderately higher than that of BTT1-3A (0.44 at $80 \mu\text{M}$) despite identical peptide net charge of +7 (Table S1, Supporting Information). This agrees with our previous analysis that variations in amphipathicity pattern of the turn sequence can considerably impact LPS-binding affinity.^[11] Vortexing of the centrifuged samples resulted in the release of most of the FITC-LPS back to the supernatant (Figure S2, Supporting Information), thus ruling out photobleaching during processing as a cause for the

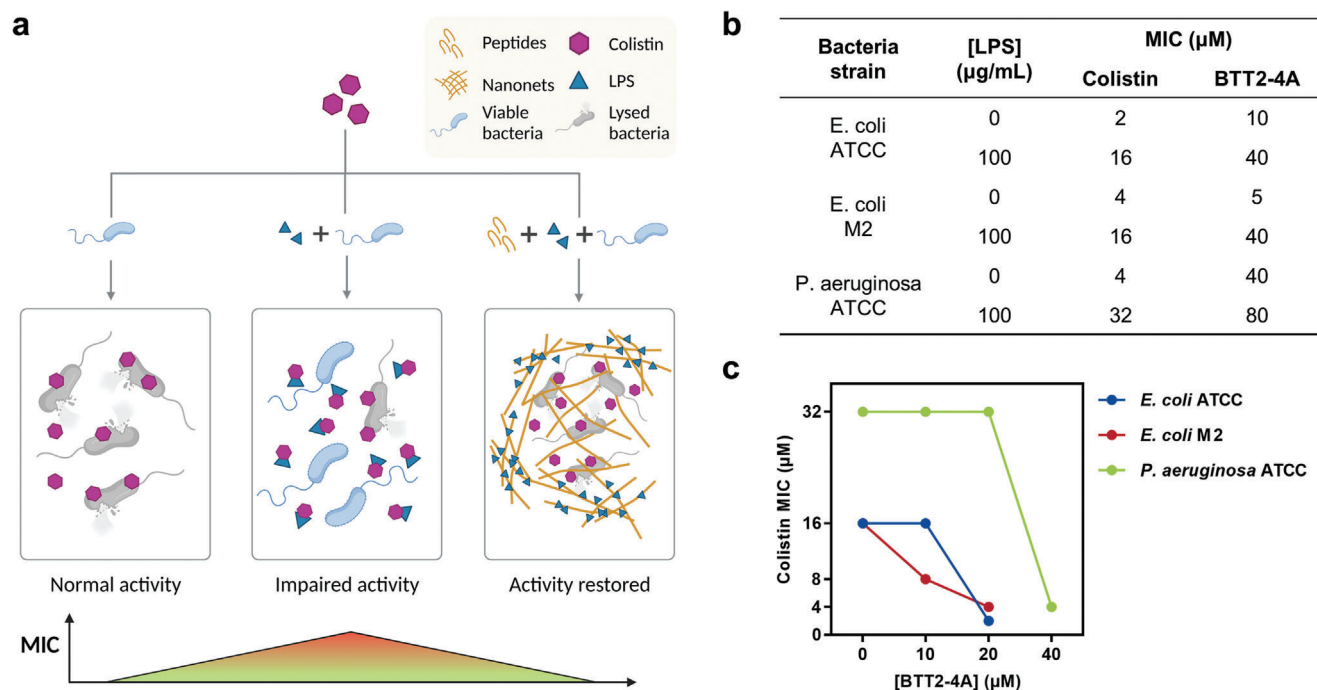


Figure 2. Peptide nanonets nullify the colistin-inactivating effect of extracellular LPS. a) Proposed mechanism of fibrillating peptide rescuing the activity of colistin. b) MICs of BTT2-4A and colistin against different bacteria strains were determined either in the absence or presence of $100 \mu\text{g mL}^{-1}$ cell-free LPS. c) MICs of colistin were determined in the presence of free LPS ($100 \mu\text{g mL}^{-1}$) and varying sub-MIC concentrations of BTT2-4A. MIC assays were conducted in duplicates in three independent experiments.

observed decrease in fluorescence signals. Confocal microscopy was used to visualize nanocomplexation between FITC-LPS and the nanonets. After 1 h of incubation with the fibrillating peptides BTT2-4A and BTT1-3A, FITC-LPS was observed to form large aggregates with intense green fluorescence (Figure 1b), whose size was comparable to FITC-labeled peptide aggregates previously observed.^[9] In contrast, incubating FITC-LPS with the non-fibrillating BTT2-2A or in the absence of peptide did not yield visible aggregates. Taken together, the findings suggest that free LPS in solution could be readily captured by peptide nanonets.

To gain mechanistic insights into the endotoxin trapping process, peptide nanonets were pre-formed during 1 h pre-incubation with non-labeled LPS, followed by exposure to FITC-LPS for quantification of trapping efficacy like above. This set-up simulates situations where administered peptides first self-assemble to form nanonets in response to bacteria cells before encountering the circulated endotoxins. Overall, trapping capacity of pre-formed nanonets increased with peptide concentration up to $\approx 50 \mu\text{M}$, above which a plateau was observed (Figure 1c). From the concentration-response curve, the LPS-trapping ability of BTT2-4A nanonets ($\text{EC}_{50} = 12.2 \mu\text{M}$) was slightly more potent than BTT1-3A ($\text{EC}_{50} = 15.1 \mu\text{M}$). K114 fluorescence assay was conducted to quantify amyloid formation during the pre-incubation period. The fluorescence dye K114 exhibits a red-shift and higher fluorescence when it binds to amyloid fibrils.^[14] BTT1-3A induced a higher K114 fluorescence than BTT2-4A at all tested concentrations (Figure S3, Supporting Information), indicating a greater amount of pre-formed nanonets during pre-incubation with non-labeled LPS. The negative cor-

relation between the quantity of pre-formed nanonets ($\text{BTT2-4A} < \text{BTT1-3A}$) and subsequent extent of FITC-LPS trapping ($\text{BTT2-4A} > \text{BTT1-3A}$) can be explained by a dual endotoxin trapping mechanism (Figure 1d): (1) scaffold integration: LPS served as amyloid-nucleating foci and was integrated within the elongating nanofibrils, and (2) post-binding: LPS was electrostatically bound to the pre-formed nanofibrils. Compared to BTT1-3A, a lesser extent of pre-formed BTT2-4A nanonets implies that more BTT2-4A molecules remained in solution for additional nanonets formation with FITC-LPS, followed by greater FITC-LPS trapping via mechanism (1). Meanwhile, more limited binding pockets on pre-formed BTT2-4A nanonets would allow for less FITC-LPS trapping via mechanism (2), assuming that the binding sites for K114 and LPS highly correlate. These sites comprise both external surfaces and internal structures of the pre-formed fibrils. Altogether, mechanism (1) appears to play a more prominent role.

We previously observed that LTA, a biomolecule characteristic of Gram-positive membranes, induced the formation of nanonets with different morphology and behaviors than LPS.^[9] To investigate whether nanonets induced by Gram-positive bacteria can also capture free LPS, we triggered pre-formed nanonets using LTA in place of LPS during the pre-incubation step, then measured the extent of FITC-LPS trapping. Overall, LTA-induced nanonets displayed an endotoxin-trapping profile very similar to LPS-induced counterparts (Figure S4, Supporting Information), thus suggesting that our nanonets can retain therapeutic utility against polymicrobial infections of both Gram-positive and Gram-negative pathogens.

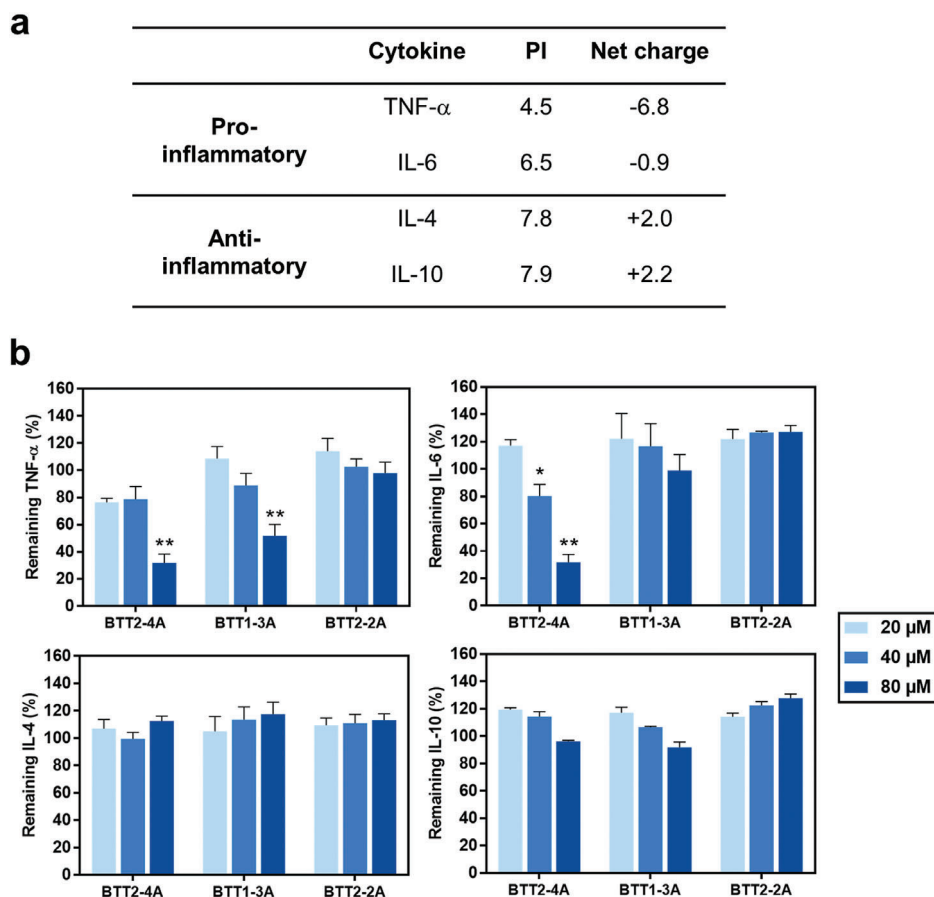


Figure 3. Peptide nanonets display selective binding toward pro-inflammatory cytokines. a) Isoelectric point (PI) and net charge of the cytokines tested in this work. b) Cytokine trapping by LPS-induced nanonets. After 1 h of incubating LPS ($5 \mu\text{g mL}^{-1}$) and cytokine (2 ng mL^{-1}) with peptide at different concentrations, sample was centrifuged and the cytokine remaining in the supernatant was quantified using ELISA. Results were normalized against peptide-free controls subjected to identical processing steps. Three independent experiments were performed in duplicates and data are presented as mean \pm SE. Statistical significance between samples were evaluated using one-way analysis of variance (ANOVA) followed by Tukey post-hoc test (*: $p \leq 0.05$, **: $p \leq 0.01$).

2.2. LPS-Trapping Activity of Nanonets Enables Restoration of Colistin Activity

Endotoxin-trapping activity of the nanonets can be utilized for various biomedical applications. Colistin is a last-resort antibiotic that disrupts bacteria membranes by interacting with membrane-bound LPS, and its activity can be impaired by competitive binding from extracellular LPS whose abundance markedly elevates during sepsis.^[8] By capturing free LPS, we hypothesized that our nanonets could safeguard colistin from their interference, thus enabling membrane interactions and antimicrobial activity by the antibiotic (Figure 2a). To this end, we employed broth microdilution method to determine the activity of colistin and peptides under different conditions, where a lower minimum inhibitory concentration (MIC) signifies more potent antimicrobial activity. Against *Escherichia coli* (*E. coli*) ATCC 25922, the individual MICs of colistin and BTT2-4A in the absence of LPS were 2 and $10 \mu\text{M}$, which increased eight- and four-fold in the presence of LPS ($100 \mu\text{g mL}^{-1}$) (Figure 2b). In combination, the addition of BTT2-4A at a sub-MIC concentration ($20 \mu\text{M}$) was observed to lower the LPS-impaired MIC of colistin eightfold from 16 to

$2 \mu\text{M}$ (Figure 2c), thus restoring colistin activity. For comparison, gold nanosheets recently reported by Liao et al. only achieved a twofold reduction in colistin MIC, but requires a very high gold concentration of $500 \mu\text{g mL}^{-1}$.^[8] BTT2-4A also exhibited similar antibiotic-potentiating effect against other Gram-negative strains. When tested with the colistin-resistant *E. coli* M2 clinical isolate and *Pseudomonas aeruginosa* ATCC 9027, BTT2-4A at sub-MIC concentrations yielded respectively four- and eight-fold decrease in LPS-impaired MIC of colistin to $4 \mu\text{M}$ (Figure 2c). The significant improvement in antibacterial potency of colistin might be explained by a threshold peptide concentration above which nanonets formation drastically increased, which in turn elevated the endotoxin-trapping capacity of the peptide.

2.3. Nanonets Selectively Bind Pro-Inflammatory Cytokines through Electrostatic Interactions

We next explored the interactions between our peptides and inflammation mediators (Figure 3a). After incubating the peptides with LPS ($5 \mu\text{g mL}^{-1}$) and recombinant murine cytokine

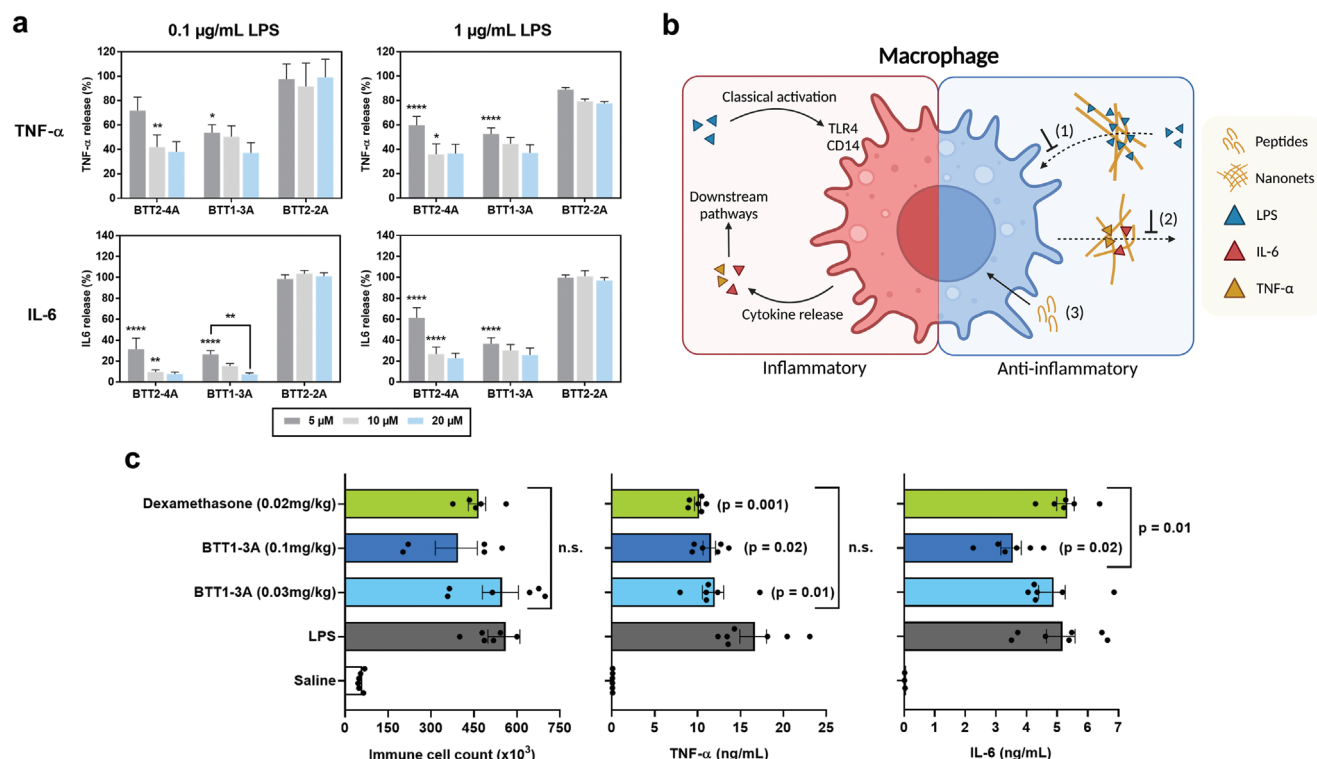


Figure 4. Peptide nanonets suppress LPS-induced release of pro-inflammatory cytokines by RAW cells. a) Effect of peptide post-treatment on LPS-induced TNF- α and IL-6 production by RAW 264.7 cells at different LPS concentrations. After 1 h of incubating the cells with LPS, peptide was added followed by 23 h incubation before cytokine in the culture media was quantified. Results were normalized against the peptide-free negative control. Three independent experiments were conducted, and data are presented as mean \pm SE. Statistical significance between samples were evaluated using one-way analysis of variance (ANOVA) followed by Tukey post-hoc test (*: $p \leq 0.05$, **: $p \leq 0.01$, ***: $p \leq 0.001$, ****: $p \leq 0.0001$). b) Proposed anti-inflammatory mechanisms of the fibrillating peptides: (1) LPS trapping by the nanonets, (2) cytokine trapping by the nanonets, and (3) intracellular effect by soluble peptide molecules. c) Quantification of immune cells and cytokine production in bronchoalveolar lavage fluids (BALF) collected from mice after 4 h treatment ($n = 5$ –6 per group). Mice were given LPS only or saline as controls. Data are presented as mean \pm SD. Statistical significance between samples were evaluated using one-way ANOVA followed by Tukey post-hoc test, and p values are shown in figure.

(2 ng mL⁻¹) for 1 h, we centrifuged the sample and quantified the amount of free cytokine remaining in supernatant using standard enzyme-linked immunosorbent assay (ELISA). Whereas the non-fibrillating BTT2-2A failed to precipitate cytokines in the pellet, the fibrillating BTT2-4A exhibited substantial cytokine-trapping ability with a clear preference for tumor necrosis factor- α (TNF- α) and interleukin-6 (IL-6), which are secreted by macrophages during systemic inflammation.^[15] At 80 μ M, BTT2-4A nanonets entrapped >70% of these two cytokines, but did not lower the quantity of free IL-4 and IL-10 in the supernatant (Figure 3b). As acutely observed by Shi et al.,^[5] pro-inflammatory cytokines (e.g., TNF- α and IL-6) mostly carry negative charges, whereas many anti-inflammatory cytokines (e.g., IL-4 and IL-10) are positively charged. The apparent trapping selectivity of our nanonets toward the pro-inflammatory cytokines is indicative of electrostatic interactions mediated by the cationic Lys residues on the peptides. Of interest, BTT1-3A at 80 μ M captured \approx 50% of TNF- α but had negligible effect on IL-6. The higher hydropathy value of BTT2-4A signifies that it is more hydrophobic than BTT1-3A (Table S1, Supporting Information). The corresponding greater binding affinity of BTT2-4A toward the near-neutral IL-6 suggests that hydrophobic interactions also contribute to cytokine-trapping activity of the nanonets. LTA-

nucleated BTT2-4A and BTT1-3A nanonets also displayed selective trapping activity toward pro-inflammatory cytokines while not affecting anti-inflammatory cytokines (Figure S4, Supporting Information), which supports the clinical potential of the nanonets against Gram-positive bacteria.

2.4. In Vitro and In Vivo Anti-Inflammatory Activity of the Peptides

We then evaluated the peptide effect on LPS-activated cytokine production by the murine macrophage RAW 264.7 cells. When LPS is recognized by the membrane-bound TLR4 and CD14 co-receptors on macrophages, signaling pathways are activated which promote the release of cytokines.^[16] When the cells were post-treated with BTT2-4A or BTT1-3A after LPS exposure, their cytokine release measured after 24 h was significantly lower than untreated control, with a more pronounced impact on IL-6 than TNF- α (Figure 4a). In contrast, treatment with the non-fibrillating BTT2-2A had minimal effect on cytokine release despite an identical net charge among the peptides (Table S1, Supporting Information). This establishes nanonet formation as a pre-requisite for mitigating LPS-induced cytokine release by

macrophages. Peptide pre-treatment 1 h before LPS was added to the media did not yield noticeably greater anti-inflammatory effect than post-treatment (Figure S5, Supporting Information). When we increased LPS concentration from 0.1 to 1 $\mu\text{g mL}^{-1}$, the percentage of cytokine release by peptide-treated macrophages remained similar. By showing that the peptides were not cytotoxic at all tested concentrations (Figure S6, Supporting Information), we could rule out lysis of the macrophages as a cause for the observed decrease in cytokine release.

Although BTT1-3A displayed considerably weaker LPS-trapping efficacy than BTT2-4A (Figure 1) and negligible trapping effect against IL-6 (Figure 3b), it was found to strongly inhibit LPS-induced IL-6 production by macrophages (Figure 4a). These findings suggest that the fibrillating peptides also have direct suppressive effect on cellular pathways governing cytokine release. We thus propose a multi-pronged anti-inflammatory mechanism which impacts the inflammation process at various stages: (1) Nanonets entrap LPS which prevents macrophage binding and activation, (2) nanonets entrap released pro-inflammatory cytokines which mitigates their ability to trigger downstream inflammatory events, and (3) monomeric peptide molecules unassociated in nanonets penetrate immune cells and inhibit intracellular cytokine release pathways.

With moderately greater in vitro anti-inflammatory activity in RAW 264.7 cells (Figure 4a and Figure S4, Supporting Information), BTT1-3A was selected for exploring in vivo efficacy. Animal experiments were performed in accordance to protocol no. R20-01283 approved by the Institutional Guidelines of the Animal Care and Use Committee at National University of Singapore. We employed an endotoxin-induced acute lung injury model in mice, whereby the mice were euthanized at 4 h post-treatment and bronchoalveolar lavage fluid (BALF) was collected post-mortem for analysis. The effect of LPS on local immune response in the mice was apparent when compared to saline control, as saline vehicle control induced minimal immune cell count and cytokine levels in BALF (Figure 4c). In mice treated with BTT1-3A via intratracheal administration, the level of pro-inflammatory cytokines TNF- α and IL-6 in BALF was significantly lowered in a concentration-dependent manner. An equimolar dose of BTT1-3A (0.1 mg kg^{-1}) achieved comparable efficacy to the positive control dexamethasone (0.02 mg kg^{-1}) at lowering TNF- α , but greater effect against IL-6 ($p = 0.02$). We also observed that neither BTT1-3A nor dexamethasone caused any change in the BALF immune cell count, which indicates a lack of effect on immune cell chemotaxis. Overall, our fibrillating peptide exhibited promising in vivo activity at reducing endotoxin-activated immune response.

3. Conclusions

In summary, our peptide nanonets displayed promising anti-inflammatory activity both in vitro and in vivo, thus expanding their repertoire of functionalities beyond that of antibacterial trap-and-kill.^[9] The nanonets are postulated to specifically bind and entrap endotoxin and pro-inflammatory cytokines by exploiting the abundance of negative charges on these inflammation mediators. This could potentially overcome the limitation in activity spectrum associated with target-specific anti-septic strategies, and minimize undesirable inactivation of the beneficial

anti-inflammatory mediators. In addition, we propose that the LPS-trapping ability of the nanonets can be mobilized as adjuvant action to nullify antagonistic interactions from extracellular LPS and restore the activity of clinically relevant antibiotics. By expanding their arsenal of functionalities, we hope to promote further development of peptide-based nanonets as multi-purpose anti-infective biomaterials.

4. Experimental Section

The full experimental procedures for this study are available in the Supporting Information.

Supporting Information

Supporting Information is available from the Wiley Online Library or from the author.

Acknowledgements

Animal experiments were approved the Institutional Animal Care and Use Committee of the University of Singapore (22/6170832). The research work described in this manuscript was conducted with facilities provided by the National University of Singapore. This work was supported by Ministry of Education (MOE) Tier 1 grant (Grant no.: A-0004347-00-00) awarded to P.L.R.E, and CREATE Program Grant A-0006243-00-00 from the National Research Foundation of Singapore and a DDOP Platform Grant E-559-00-0004-01 from the National University Health System (NUHS) awarded to W.S.F.W.

Conflict of Interest

The authors declare no conflict of interest.

Data Availability Statement

The data that support the findings of this study are available from the corresponding author upon reasonable request.

Keywords

anti-infective, anti-septics, inflammation, nanostructures, peptides

Received: December 12, 2022
Revised: March 8, 2023
Published online: April 25, 2023

- [1] S. R. Finfer, J.-L. Vincent, D. C. Angus, T. Van Der Poll, *N. Engl. J. Med.* **2013**, 369, 669.
- [2] M. Yaroustovsky, M. Plyushch, D. Popov, N. Samsonova, M. Abramyan, Z. Popok, N. Krotenko, *J. Inflammation* **2013**, 10, 8.
- [3] L. Gabrielli, A. Capitoli, D. Bini, F. Taraballi, C. Lupo, L. Russo, L. Cipolla, *Curr. Drug Targets* **2012**, 13, 1458.
- [4] B. G. Chousterman, F. K. Swirski, G. F. Weber, *Semin. Immunopathol.* **2017**, 39, 517.

- [5] C. Shi, X. Wang, L. Wang, Q. Meng, D. Guo, L. Chen, M. Dai, G. Wang, R. Cooney, J. Luo, *Nat. Commun.* **2020**, *11*, 3384.
- [6] S. Thamphiwatana, P. Angsantikul, T. Escajadillo, Q. Zhang, J. Olson, B. T. Luk, S. Zhang, R. H. Fang, W. Gao, V. Nizet, L. Zhang, *Proc. Natl. Acad. Sci. U. S. A.* **2017**, *114*, 11488.
- [7] D. S. S. M. Uppu, Y. Min, I. Kim, S. Kumar, J. Park, Y. K. Cho, *ACS Appl. Mater. Interfaces* **2021**, *13*, 29313.
- [8] F.-H. Liao, T.-H. Wu, C.-N. Yao, S.-C. Kuo, C.-J. Su, U.-S. Jeng, S.-Y. Lin, *Angew. Chem., Int. Ed. Engl.* **2020**, *59*, 1430.
- [9] N. D. T. Tram, J. Xu, D. Mukherjee, A. E. Obanel, V. Mayandi, V. Selvarajan, X. Zhu, J. Teo, A. Barathi, R. Lakshminarayanan, P. L. R. Ee, *Adv. Funct. Mater.* **2022**, *33*, 2210858.
- [10] H. Chu, M. Pazgier, G. Jung, S.-P. Nuccio, P. A. Castillo, M. F. de Jong, M. G. Winter, S. E. Winter, J. Wehkamp, B. Shen, N. H. Salzman, M. A. Underwood, R. M. Tsois, G. M. Young, W. Lu, R. I. Lehrer, A. J. Baumbler, C. L. Bevins, *Science* **2012**, *337*, 477.
- [11] N. D. T. Tram, V. Selvarajan, A. Boags, D. Mukherjee, J. K. Marzinek, B. Cheng, Z. C. Jiang, P. Goh, J. J. Koh, J. W. P. Teo, P. J. Bond, P. L. R. Ee, *Acta Biomater.* **2021**, *135*, 214.
- [12] K. Nishio, M. Horie, Y. Akazawa, M. Shichiri, H. Iwahashi, Y. Hagi-hara, Y. Yoshida, E. Niki, *Redox Biol.* **2013**, *1*, 97.
- [13] I. Zanoni, R. Ostuni, L. R. Marek, S. Barresi, R. Barbalat, G. M. Barton, F. Granucci, J. C. Kagan, *Cell* **2011**, *147*, 868.
- [14] A. S. Crystal, B. I. Giasson, A. Crowe, M.-P. Kung, Z.-P. Zhuang, J. Q. Trojanowski, V. M.-Y. Lee, *J. Neurochem.* **2003**, *86*, 1359.
- [15] T. Hirano, *Int. Immunol.* **2021**, *33*, 127.
- [16] B. S. Park, D. H. Song, H. M. Kim, B. S. Choi, H. Lee, J. O. Lee, *Nature* **2009**, *458*, 1191.